Intermolecular rovibrational bound states of H_2O-H_2 dimer from a MultiConfiguration Time Dependent Hartree approach

Steve A. Ndengué

Department of Chemistry, Missouri University of Science and Technology, 65409 Rolla, Missouri, United States.

Yohann Scribano

Laboratoire Univers et Particules de Montpellier, UMR-CNRS 5299, Université de Montpellier, Place eugène Bataillon, 34095 Montpellier Cedex, France.

David M. Benoit

E.A. Milne Centre for Astrophysics & G.W. Gray Centre for Advanced Materials, Chemistry, The University of Hull, Cottingham Road, Kingston upon Hull HU6 7RX, United Kingdom

Fabien Gatti

Institut de Sciences Moléculaires d'Orsay, UMR-CNRS 8214, Université Paris-Sud - Université Paris-Saclay, 91405 Orsay, France.

Richard Dawes

Department of Chemistry, Missouri University of Science and Technology, 65409 Rolla, Missouri, United States.

Abstract

We compute the rovibrational eigenstates of the H_2O-H_2 Van der Waals complex using the accurate rigid-rotor potential energy surface of Valiron *et al.* [J. Chem. Phys. **129**, 134306 (2008)] with the MultiConfiguration Time Dependent Hartree (MCTDH) method. The $J = 0 - 2$ rovibrational bound states calculations are done with the Block Improved Relaxation procedure of MCTDH and the subsequent assignment of the states is achieved by inspection of the wavefunctions' properties. The results of this work are found to be in excellent agreement with previous time independent calculations reported for this complex and therefore confirms the high accuracy as well as efficiency of the MCTDH approach for the rovibrational spectroscopic study of such weakly bound complexes.

Keywords: Quantum Dynamics, Bound states, Time-dependent, Van der Waals, MCTDH

1. Introduction

Simulating material properties from first principles at the molecular level is a very challenging goal for all technological materials development or for a more fundamental perspective. This may require an accurate *ab initio* potential energy surface (PES) which should be accurate enough to be used for a large range of applications starting from gas-phase to the study of the bulk-phase properties. For many years, the field of van der Waals molecules, or weakly bound complexes (implying non-covalent bonding between atoms), has emerged and their molecular spectroscopic properties (like tunneling splittings in water clusters) have been used to test or/and develop accurate many-body PESs. Usually those molecular cluster PESs are expanded as a sum of low-order many body terms[1, 2, 3, 4, 5, 6, 7]. It was shown that including up to three-body terms is enough to correctly reproduce the infrared and Raman spectrocopy of liquid water[8, 9]. The accuracy of the *ab initio* two-body term, the dimer potential, may be evaluated by a direct comparison between observed experimental spectrum and theoretical spectrum obtained by solution of the Schrödinger equation as was done recently in the study of the water dimer[10, 11].

The H_2O-H_2 van der Waals complex is an example of a molecular dimer with relevance in domains beyond chemical physics. It is indeed an important system within the astrophysical context since H_2O is the third most abundant polyatomic system after CO and H_2. Thus the complex involves two of the most abundant molecules in the Interstellar Medium (ISM), which are also important on Earth. The knowledge of an accurate PES is thus required in order to determine the efficiency of the molecular (H_2O) cooling through its inelastic collisions with molecular hydrogen [12, 13, 14, 15, 16, 17]. This van der Waals complex is also of interest for gas storage materials such as hydrogen clathrate hydrates[18, 19, 20] due to their potential

as efficient and environmentally friendly materials for hydrogen storage. Indeed, most of the theoretical studies of one or more H_2 molecules encapsulated in clathrate hydrate make the assumption that the interaction between the guest molecule and the host ice-water structure can be described as a sum of pairwise water-hydrogen dimer interactions[21, 22].

The quantum dynamics of H_2O-H_2 is complicated by the inherently large amplitude motions which characterize weakly-bounded complexes with light-atoms and their associated large zero-point-energies (ZPE). All intermolecular motions are delocalized over the various minima of the PES. The previous theoretical spectroscopy studies have used a time-independent approach to solve the Schrödinger nuclear equation and compute the rovibrational bound states within the rigid rotor model. Those previous spectroscopic calculations have been performed by Wang and Carrington [23] using a combination of Discrete Variable Representation (DVR) and Finite Basis Representation (FBR) with Lanczos diagonalization as well as by Avoird[24] who used a Close Coupling (CC) methodology combined with a Davidson algorithm to determine the rovibrational states. Those two time independent calculations have also used the accurate five dimensional *ab initio* potential of Valiron *et al.*[25] which was obtained from the original nine-dimensional potential energy surface by averaging over the intramolecular vibrational ground state probability densities of water and hydrogen.

In this work, we describe the numerical solution of the rovibrational Schrödinger equation for this complex using an efficient time-dependent method: the MCTDH approach. This approach was recently used by Ndengué *et al.*[26] in an inelastic scattering study of the Ar-H_2O atom-triatom complex and has demonstrated remarkable accuracy in comparison to CC calculations on this same system. This work on the water-hydrogen complex is an immediate continuation of the previous work and represents the first application of the MCTDH methodology for the rovibrational spectroscopy of a diatomic-triatomic system.

This article is organized as follows: first we will discuss the computational procedure, introducing the MCTDH method, the Hamiltonian (kinetic operator and the potential energy surfaces) and how the rovibrational states calculations are done. Next we will present and discuss our results and conclude with perspectives.

2. Computational procedure

2.1. Rigid Body diffusion monte carlo calculations

In order to benchmark the ground state calculation, we have performed the ground state calculation of the *para-para* H_2O–H_2 complex using Diffusion Monte Carlo (DMC). Indeed, this is a practical method to solve accurately the many-body vibrational Schrödinger equation and is particularly suited to the determination of the vibrational ground state. DMC replaces the resolution of the

time-independant Schrödinger equation by the simulation of a diffusion process in imaginary time $\tau = it$ on a given multidimensional PES. In particular, DMC avoids the convergence problems that can be encountered in discrete-variable representation or in spectral approaches due to the finite basis set representation, and thus is often used as a reference method to provide benchmark values. We use the rigid-body version of DMC (RB-DMC), initially proposed by Buch [27], and used by other authors [28, 29] to compute the vibrational ground state of weakly bounded clusters. For these molecular systems, decoupling the fast intramolecular modes from the slow intermolecular modes is a very good approximation and we can consider each rotor as a rigid body since this approximation was already validated in the case of water dimers[30]. Our RB-DMC simulations are performed with the XDMC code developed by Benoit[31] (see also Ref. [32] for implementation details). In this study we use 500 replicas, a stabilization period of 11×100 cycles with $\Delta\tau = 30$ a.u. and an averaging phase of 2000×100 cycles with $\Delta\tau = 5$ a.u. We get a RB-DMC vibrational ground state of -33.58 ± 0.16 cm^{-1} in very good agreement with the previous values of Wang and Avoird. The water–hydrogen system is indeed strongly anharmonic and has a very weakly bound vibrational ground state.
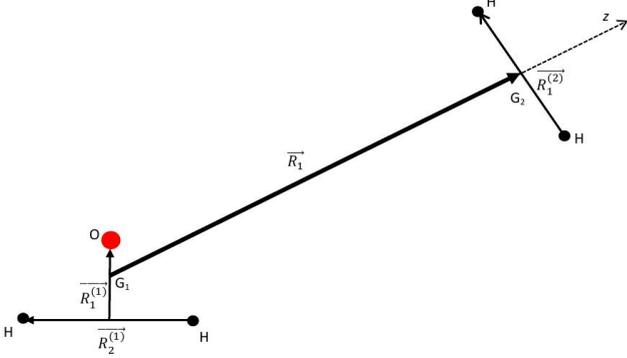
2.2. The MCTDH method

The MultiConfiguration Time Dependent Hartree [33, 34] method is a time-dependent method in which each degree of freedom is associated with a small number of orbitals or single particle functions (SPFs) which, through their time dependence, allow efficient description of the molecular dynamical processes. The total MCTDH wave function is expanded in Hartree products, that is, products of single-particle functions

$$\Psi(Q_1,\ldots,Q_f,t) = \sum_{j_1=1}^{n_1} \cdots \sum_{j_f=1}^{n_f} A_{j_1\cdots j_f}(t) \prod_{\kappa=1}^{f} \phi_{j_\kappa}^{(\kappa)}(Q_\kappa,t)$$

$$= \sum_J A_J \Phi_J, \qquad (1)$$

where f is the number of degree of freedom of the system, $Q_1,\ldots,Q_f$ are the nuclear coordinates, $A_{j_1\cdots j_f}$ denotes the MCTDH expansion coefficients, and $\phi_{j_\kappa}^{(\kappa)}(Q_\kappa,t)$ are the n_κ SPFs associated with each degree of freedom κ. The subsequent equation of motion for the coefficients and single particle functions are derived after replacing the wave function *ansatz* into the time dependent Schrödinger equation. To solve the equations of motion, the κ SPF are represented on a primitive basis or discrete variable representation (DVR) grid of N_κ points,

$$\varphi_{j_\kappa}^{(\kappa)}(Q_\kappa,t) = \sum_{i_\kappa=1}^{N_\kappa} c_{i_\kappa j_\kappa}^{(\kappa)}(t) \chi_{i_\kappa}^{(\kappa)}(Q_\kappa) \qquad (2)$$

Figure 1: Definition of the Jacobi vectors for the H_2O-H_2 dimer. G_j is the center of mass of the jth monomer. $\vec{R_1}$ joins the center of mass of G_1 and G_2 and defines the $z-axis$. In the current calculations the $R_i^{\vec{(j)}}$ vectors have fixed lengths.

where in general the n_κ of Equation (1) is such that $n_\kappa < N_\kappa$. Thus, the MCTDH method propagates a wave function on a small time-dependent, variationally optimized basis set of single-particle functions, which in turn are defined on a time-independent primitive basis set.

2.3. The Kinetic Energy Operator

For the MCTDH algorithm to be efficient, the Hamiltonian operator must be written as a sum of products (SOP) of single-particle operators. The Kinetic Energy Operator (KEO) has always the required form when using polyspherical coordinates, such as the Jacobi coordinates used in this work where we followed the approach of Ref.35 the subsystem KEO derivation presented by Gatti and Iung[36] which was used recently to describe an asymmetric rotor – atom collision[26]. As was the case with previous MCTDH calculations involving fragments, we do not work in the Body-Fixed frame but in the E_2 frame[36] which is obtained by rotation of the two first Euler angles of the SF frame. A choice of the vectors for this calculation is displayed in Figure 1. The KEO in the E_2 frame is generally expressed as

$$
\begin{aligned}
2\hat{T} \quad &= -\frac{1}{\mu_R}\frac{\partial^2}{\partial R^2} + 2\hat{T}_A + 2\hat{T}_B \\
&+ \frac{1}{\mu_R R^2}\left(\vec{J}^\dagger\vec{J} + (\vec{L}_A + \vec{L}_B)^2 - 2(\vec{L}_A + \vec{L}_B)\vec{J}\right)_{E_2}
\end{aligned} \tag{3}
$$

where μ_R is the reduced mass of the H_2O–H_2 cluster, the A and B subscripts refer respectively to the H_2O and H_2 fragments. J, L_A and L_B are respectively the total angular momentum of the system and the angular momenta of the fragments A (H_2O) and B (H_2). The rigid rotor

Hamiltonian of the H_2O molecule is expressed as[37]

$$
\begin{aligned}
\hat{T}_A \quad &= \frac{A}{2}\left(L_{A,+}^2 + L_{A,-}^2 + L_{A,+}L_{A,-} + L_{A,-}L_{A,+}\right) \\
&- \frac{C}{2}\left(L_{A,+}^2 + L_{A,-}^2 - L_{A,+}L_{A,-} - L_{A,-}L_{A,+}\right) \\
&+ B L_{z_{BF_A}}^2,
\end{aligned} \tag{4}
$$

where the rotational constants have values $A = 27.8572$ cm^{-1}, $B = 14.5145$ cm^{-1} and $C = 9.2799$ cm^{-1}. The rigid rotor kinetic energy of the H_2 fragment is written simply as $\hat{T}_B = B_{H_2}\vec{L}_B^2$ where the rotational constant $B_{H_2} = 59.2434$ cm^{-1}. The final form of the KEO translated and implemented in the MCTDH code is then

$$
\begin{aligned}
2\hat{T} \quad &= -\frac{1}{\mu_R}\frac{\partial^2}{\partial R^2} + 2\hat{T}_A + 2\hat{T}_B \\
&+ \frac{1}{\mu_R R^2}\left(J(J+1) + \vec{L}_A^2 + \vec{L}_B^2 - 2L_{A,z}^2 - 2L_{B,z}^2\right) \\
&+ \frac{1}{\mu_R R^2}\left(L_{A,+}L_{B,-} + L_{A,-}L_{B,+} - 2L_{A,z}L_{B,z}\right) \\
&+ \frac{1}{\mu_R R^2}\left(C_+(J,K)(L_{A,+} + L_{B,+})\right) \\
&+ \frac{1}{\mu_R R^2}\left(C_-(J,K)(L_{A,-} + L_{B,-})\right),
\end{aligned} \tag{5}
$$

with

$$
L_{A(B),\pm} = L_{A(B),x} \pm iL_{A(B),y}, \tag{6}
$$

and

$$
C_\pm(J,K) = \sqrt{(J(J+1) - K(K \pm 1)}. \tag{7}
$$

2.4. The Potential Energy Surface

The potential energy operator just as the KEO needs to be expressed in the product form. For systems of low dimensionality which are not already in the product form, there exists an efficient fitting procedure (Potfit)[38, 39] implemented in the MCTDH package[40] to obtain the desired representation. For high dimensionality potentials MultiGrid[41], Multi-Layer[42] and Monte Carlo[43] versions exist to transform a general potential to the product form. However those implementations often lead to a large number of potential terms which will slow down the computations, for example in scattering calculations where several long propagations are necessary to obtain the cross-sections. In this work, we are able to go around this difficulty since the potential[25] is already provided in a multipolar form and we only had to make a transformation to express it in the coordinates representation used for the MCTDH calculations.

The surface from Ref.25 is expressed as

$$
V(R,\theta,\varphi,\theta',\varphi') = \sum_i v_i(R)\bar{t}_i(\theta,\varphi,\theta',\varphi') \tag{8}
$$

where $i = \{l_A, m_A, l_B, l\}$ and $\bar{t}_{l_A, m_A, l_B, l}$ is expressed as

$$\bar{t}_i(\theta, \theta', \varphi, \varphi') = \frac{1}{2\pi} \alpha_{l_A, m_A} \sum_{r_1=-l_A}^{l_A} \sum_{r_2=-l_B}^{l_B} \beta_{i, r_1} \begin{pmatrix} l_A & l_B & l \\ r_1 & r_2 & r \end{pmatrix}$$
$$\times \left(P_{l_B}^{r_2}(cos\theta') P_l^r(cos\theta) cos(r_2\varphi' + r\varphi) \right) \tag{9}$$

with

$$\alpha_{l_A, m_A} = \frac{\sqrt{2l_A + 1}}{\sqrt{2 + 2\delta_{m_A, 0}}}, \tag{10}$$

and

$$\beta_{i, r_1} = \frac{1}{2\pi} \left(\delta_{m_A, r_1} + (-1)^{l_A + m_A + l_B + l} \delta_{-m_A, r_1} \right). \tag{11}$$

The maximum order of the terms involved in the expansion are $l_A = 11$, $l_B = 6$, resulting in 149 $v_i(R)$ terms in equation (8) with $m_A (\geq 0)$, l_A and $l_A + l_B + l$ always even because of symmetry considerations. The BF of the original PES is defined such that its origin is the center of mass of the H_2O molecule, the $z - axis$ is its C_2 axis with the positive z in the direction of the O atom and the xz plane is the molecular plane. The angles (θ, φ) and (θ', φ') represent respectively the collisional direction and the H_2 fragment orientation in the Body-Fixed (BF) frame. In the MCTDH implementation, the dynamics in the E_2 frame is described by 6 coordinates, R the fragments' separation and 5 angles: α_A, β_A, γ_A, θ_B and ϕ_B. The origin of the E_2 frame is the center of mass of H_2O as was the case with the BF frame. The $z - axis$ is the axis of $\vec{R}$, the connecting vector between the centers of mass of H_2O and H_2. The 3 Euler angles α_A, β_A, γ_A give the orientation of of H_2O in our frame while the other 2 spherical angles θ_B and ϕ_B give the orientation of the H_2 fragment. We point out that the BF Frame and the E_2 Frame mentioned here correspond respectively to the Molecule Fixed (MF) Frame and the Dimer Fixed (DF) Frame described in the work of Wang and Carrington [23]. A cut of the PES expressed in the set of coordinates used by Valiron *et al* is shown in Figure 2.

As Van der Avoird and Nesbitt[24] noticed, there are two ways to transform the PES from the MF Frame set of coordinates to DF Frame set of coordinates. In the first approach the coordinates are related according to $\theta = \beta_A$, $\varphi = \pi - \gamma_A$ and θ', φ' can be expressed in terms of $\alpha_A, \beta_A, \gamma_A, \theta_B, \phi_B$ with the use of the inverse Euler rotation matrix; then the PES in the appropriate frame can be numerically generated. This procedure, used by Wang and Carrington,[23] is not convenient for this work as it would require to build a new SOP expansion of the PES after the surface is numerically transformed. The second approach,[24] which is the one we selected, relates the co-efficients of the multipolar expansion in both frames and thus allows one to generate the PES exactly in the E_2 Frame directly in the SOP form. The correctness of the

Figure 2: 2D cut of the PES in the set of coordinates used by Valiron *et al*[25]. The figure shows the global and secondary minima of the PES.
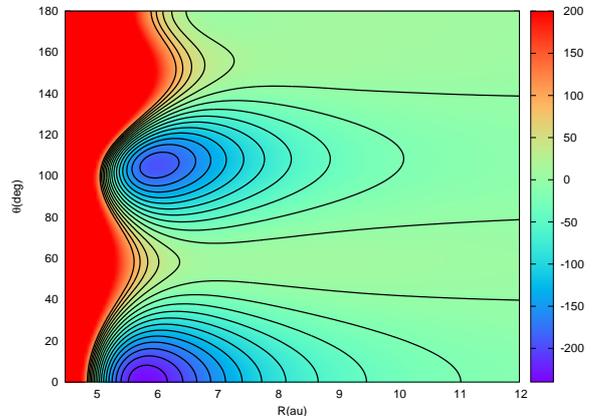
multipolar expansion can then be verified by comparison of the PES values with the ones generated from the first approach. This second approach saves a significant amount of time and allows a lot of flexibility in the calculations.

2.5. Rovibrational states calculations with MCTDH

The rovibrational bound states of the H_2O–H_2 complex are obtained with the block improved relaxation method[44, 33], implemented in the MCTDH package[40]. The block improved relaxation is derived from the improved relaxation method[45], an MCSCF approach where the SPFs are optimized by relaxation[46] (propagation in imaginary time) and the coefficients vector (A-vector) is determined by diagonalization of the Hamiltonian matrix evaluated in the set of SPFs. The working equations of the improved relaxation and block improved relaxation have already been presented elsewhere[47, 33] and thus aren't given here.

The primitive basis, its range and the number of the SPFs used for the calculations of the rovibrational states are summarized in Table 1. We see that not more than 48,000 Single Particle Functions are used to run the calculations. As the calculation method is the Block Improved Relaxation, we have to perform several of those to obtain the complete set of expected rovibrational levels. Each calculation for a block of 6 functions with 48,000 SPFs and using 32 processors on a Linux based cluster takes approximately 48 hours. While the time for each calculation is not very long, the blocks are typically done sequentially, waiting for each block to complete (or be near completed) before starting the next block of higher states: this procedure adds to the overall duration of the calculation which therefore could even take longer than traditional time-independent calculations, depending on the number

4

of desired states. However, quite often in this type of application, one is interested only in a limited number of low lying states making this procedure advantageous. A primitive basis composed of Fast Fourier Transform (FFT) functions for the intermolecular distance R was coupled with a Wigner-DVR[37] basis where α_A, γ_A are replaced by their momentum representation k_α, k_γ and a two dimensional extended Legendre-K DVR[48] (replacing ϕ_B by k_ϕ) to describe respectively the orientation of the H_2O and the H_2 fragments in the E_2 frame. The Wigner and Legendre-K DVRs switch between their respective FBR (Wigner and Spherical harmonics) and DVR to calculate the action of the derivatives of operators (and the singularities) and to evaluate the potential respectively. Leforestier[37] defined the unitary transformation that goes from the 3D DVR to the 3D FBR: this transformaton is what is implemented in the MCTDH code for the Wigner-DVR, and a 2D version for the Legendre-K DVR. For testing purposes, we also ran ($J = 0$) calculations with the angular primitive basis composed of the "usual" Wigner-DVR basis and a two dimensional Legendre DVR. The (Wigner,K,K) and (KLeg,K) DVRs are then replaced by their counterparts the (Wigner,Exp,Exp) and (PLeg,Exp) DVRs, where KLeg and PLeg are respectively the extended Legendre DVR and two dimensional Legendre DVR. Results of the two sets of calculations were confirmed to be identical, with the second set running faster than the first one. However that approach is not yet implemented in the MCTDH package for $J > 0$: thus, in the rest of this work we used only the first method for our calculations.

After transforming the PES from Equation (8) to the E_2 frame we can write

$$V(R, \beta_A, \gamma_A, \alpha_A, \theta_B, \phi_B) = \sum_{\substack{r_\beta, r_\gamma \\ r_\alpha, r_\theta}} \tilde{V}_{\substack{r_\beta, r_\gamma \\ r_\alpha, r_\theta}}(R) f_{\substack{r_\beta, r_\gamma \\ r_\alpha, r_\theta}}(\omega_A, \omega_B) \tag{12}$$

where

$$f_{\substack{r_\beta, r_\gamma \\ r_\alpha, r_\theta}}(\omega_A, \omega_B) = D^{(r_\beta)}_{r_\alpha r_\gamma}(\alpha_A, \beta_A, \gamma_A)^\star C_{r_\theta, -r_\alpha}(\theta_B, \phi_B) \tag{13}$$

with D and C being respectively the Wigner D-matrix and the Racah normalized spherical harmonics. The action of the potential on the wavefunction can then be obtained using k_α, k_γ and k_ϕ to express the angles α_A, γ_A and ϕ_B, where in the following we drop the indices A and B for simplicity.

$$\hat{V}\Psi(R, \beta, k_\gamma, k_\alpha, \theta, k_\phi) = \sum_{\substack{r_\beta, r_\gamma \\ r_\alpha, r_\theta}} \bar{V}_{\substack{r_\beta, r_\gamma \\ r_\alpha, r_\theta}}(R, \beta, k_\gamma, k_\alpha, \theta, k_\phi)$$
$$\times \Psi(R, \beta, k_\gamma - r_\gamma, k_\alpha - r_\alpha, \theta, k_\phi + r_\alpha). \tag{14}$$

The primitive basis set was selected from previous work [23] done on this system for which a convergence of the results to 0.002 cm^{-1} or less for the low lying states was re-

Table 1: Parameters of the primitive basis used for the rovibrational calculations of H_2O-H_2. FFT stands for the Fast Fourier Transform. Wigner stands for the Wigner DVR. KLeg is the extended Legendre DVR. The units for distance and angle are bohrs and radians respectively.

Coords.	Primitive Basis	Number of Points	Range	SPF basis
R	FFT	96	4.0–26.0	10-20
β	Wigner	9	0–π	20-80
γ	K	17	-8,8	
α	K	17	-8,8	
θ	KLeg	9	0-π	20-30
ϕ	K	17	-8,8	

ported. Also, the number of SPFs was increased in the calculations from a relatively small number for the lower levels to significantly higher values for higher excited states. This however presents a challenge since currently symmetry is not implemented for the Wigner primitive basis in the MCTDH package. The calculations for *para/ortho* H_2O and H_2 were done without differentiating these states and the results we obtained were general and did not separate bound from resonance states for the various symmetries. For this work we will only address bound states of this system as reliable data are available for comparison. The calculations of resonances will be described and discussed in future work where we will take advantage of a recently presented procedure to obtain resonances with MCTDH[49].

3. Results and discussion

3.1. Rovibrational states and symmetry

The rovibrational states of the H_2O-H_2 cluster for $J = 0, 1, 2$ were computed with the method described above. For this work the assignment was straightforward as two sets of data[23, 24] (obtained with the same PES) which agreed very well with our calculations are already available in the literature and thus served as reference for the assignment. Comparisons of our calculations with previous results are displayed in Tables 3, 4, 5 and 6. It is worth pointing out that the difference between the two sets of previous results probably arise from the difference in the rotational constants values used by each group of authors; in our work we used the values used by Wang and Carrington[23]. Note also that their computed pH$_2$O-pH$_2$ ground state also agrees well with our RB-DMC results.

As described previously, the assignment of states resulting from MCTDH calculations (at least in its current implementation) while not trivial, is about as difficult as it is with other methods for rigid rotor Van der Waals systems. Though the calculations that were performed here did not include the symmetries of the dimer, it is possible

Table 2: Convergence of the rovibrational energies (cm^{-1}) of H$_2$O-H$_2$ for $J = 0$. The results are displayed for various SPF basis and reported as $n_1/n_2/n_3$ where the n_i are the number of SPF functions for R, (β,γ,α), (θ,ϕ).

10/40/20	20/60/25	20/70/30	10/80/30	20/90/40
-33.551	-33.562	-33.562	-33.563	-33.563
-12.826	-12.845	-12.845	-12.845	-12.846
-7.412	*-7.418*	*-7.421*	*-7.421*	*-7.421*
-7.412	*-7.418*	*-7.421*	*-7.421*	*-7.421*
-2.057	-2.064	-2.064	-2.064	-2.064
1.418	*1.411*	*1.411*	*1.411*	*1.411*

within the MCTDH code to implement and use symmetry of the Wigner-DVR and KLeg-DVR and thus run 4 separate type of calculations to treat the specific pH$_2$O-pH$_2$, pH$_2$O-oH$_2$, oH$_2$O-pH$_2$ and oH$_2$O-oH$_2$ cases presented in previous work. Thus in our computations, amongst the results, we expected to obtain the real bound states for some cases along with resonances from other cases as we do successive block improved relaxation calculations. In previous work by van der Avoird and Nesbitt[24] or Wang and Carrington[23], the primitive basis was constrained such that K, the projection of the total angular momentum writes $K = m_A + m_B$. Then, for example, $K = 0$ requires $m_A = -m_B$ and all the states that will result from their rovibrational calculations will present those characteristics. While this type of constraint is difficult to implement within the MCTDH program, it is still possible to obtain from the results of our calculations the rovibrational states that fullfill those conditions for a specific J and K and discard the other dummy states (with $J = 0$ and $K = m_A + m_B = \pm1$ for example) which may also appear in the calculations. We show in Table 2 the convergence of the first few states for $J = 0$, an output from the MCTDH calculations. We use for these calculations a primitive basis which is similar in its range and size to the results reported by Wang and Carrington[23], but where we varied the number of SPFs. We can see from the Table the convergence of the calculation, but also the dummy (or spurious) states in italic, as mentioned earlier.

The results of the rovibrational calculations from the Heidelberg MCTDH program provide relevant information that can be used to assign the various states. First, it is possible to remove spurious or non-physical rovibrational states (as we mentioned before) with $\langle m_A \rangle + \langle m_B \rangle > J$ from the calculations by individually analysing each state, doing for example a short time single-state calculation. The value of $\langle m_A \rangle + \langle m_B \rangle$ allows also one to determine the character of the rovibrational state (Σ, Π, Δ, ...). It is worth pointing out that for our calculations we didn't notice any spurious states but for another system (H$_2$O-HCN) currently being investigated this check is relevant. Secondly, in a block calculation where no use of symmetry

Table 3: Rovibrational energy levels (cm^{-1}) of pH$_2$O-pH$_2$ for $J = 0,1,2$. The parity (P) e and o stand for even and odd respectively. The character and dominant $j_{k_a k_c}$ are expressed as $\Lambda(j_{k_a k_c})$ where Λ can be Σ, Π, Δ for $K = 0$, 1, 2 (see text for details). Comparisons are made with other calculations reported for the same PES: Wang & Carrington[23] and Van der Avoird & Nesbitt[24]. Energies are in cm^{-1}.

P	$\Lambda(j_{k_a k_c})$	Ref. [23]	Ref. [24]	This Work
		$J = 0$		
e	$\Sigma(0_{00})$	-33.576	-33.567	-33.563
e	$\Sigma(0_{00})$	-2.064	-2.062	-2.064
		$J = 1$		
o	$\Sigma(0_{00})$	-32.194	-32.184	-32.181
o	$\Sigma(0_{00})$	-1.400	-1.398	-1.398
		$J = 2$		
e	$\Sigma(0_{00})$	-29.443	-29.433	-29.430
e	$\Sigma(0_{00})$	-0.163	-0.163	-0.156

Table 4: Same as Table 3 for oH$_2$O-pH$_2$.

P	$\Lambda(j_{k_a k_c})$	Ref. [23]	Ref. [24]	This Work
		$J = 0$		
e	$\Sigma(1_{01})$	-12.850	-12.834	-12.846
o	$\Sigma(1_{10})$	15.618	15.657	15.638
e	$\Sigma(1_{01})$	21.939	21.946	21.944
		$J = 1$		
o	$\Sigma(1_{01})$	-12.071	-12.055	-12.065
e	$\Pi(1_{01})$	-6.077	-6.062	-6.058
o	$\Pi(1_{01})$	-5.452	-5.437	-5.435
e	$\Pi(1_{10})$	6.951	6.992	6.963
o	$\Pi(1_{10})$	7.314	7.355	7.325
e	$\Sigma(1_{10})$	17.300	17.339	17.320
o	$\Sigma(1_{01})$	21.885	21.891	21.897
e	$\Pi(1_{01})$	22.961	22.967	22.963
o	$\Pi(1_{01})$	23.614	23.619	23.613
		$J = 2$		
e	$\Sigma(1_{01})$	-10.261	-10.245	-10.253
o	$\Pi(1_{01})$	-3.367	-3.352	-3.349
e	$\Pi(1_{01})$	-1.759	-1.744	-1.743
o	$\Pi(1_{10})$	9.073	9.114	9.085
e	$\Pi(1_{10})$	10.094	10.135	10.105
o	$\Sigma(1_{10})$	20.579	20.618	20.598
e	(1_{01})	22.524	22.529	22.525

Table 5: Same as Table 3 for pH$_2$O-oH$_2$.

P	$\Lambda(j_{k_a k_c})$	Ref. [23]	Ref. [24]	This Work
		$J = 0$		
e	$\Sigma(0_{00})$	64.879	65.083	64.892
e	$\Sigma(0_{00})$	109.911	110.115	109.913
e	$\Sigma(1_{11})$	115.120	115.335	115.075
o	$\Sigma(1_{11})$	117.733	117.956	117.958
		$J = 1$		
o	$\Sigma(0_{00})$	66.294	66.498	66.307
o	$\Pi(0_{00})$	80.176	80.378	80.233
e	$\Pi(0_{00})$	80.217	80.419	80.274
o	$\Sigma(0_{00})$	110.897	111.100	110.898
e	$\Pi(1_{11})$	111.370	111.585	111.378
o	$\Pi(1_{11})$	111.442	111.656	111.439
o	$\Sigma(1_{11})$	116.408	116.623	116.448
e	$\Pi(0_{00})$	117.361	117.561	117.393
o	$\Pi(0_{00})$	117.609	117.807	117.616
		$J = 2$		
e	$\Sigma(0_{00})$	69.114	69.318	69.127
e	$\Pi(0_{00})$	82.910	83.112	82.966
o	$\Pi(0_{00})$	83.031	83.232	83.086
e	$\Sigma(0_{00})$	112.766	112.966	112.770
o	$\Pi(1_{11})$	113.602	113.816	113.610
e	$\Pi(1_{11})$	113.761	113.974	113.756
o	$\Pi(0_{00})$	118.451	118.654	118.566

Table 6: Same as Table 3 for oH$_2$O-oH$_2$.

P	$\Lambda(j_{k_a k_c})$	Ref. [23]	Ref. [24]	This Work
		$J = 0$		
e	$\Sigma(1_{01})$	93.685	93.895	93.676
o	Σ	98.380	98.595	98.730
e	$\Sigma(1_{01})$	114.211	114.424	114.854
o	$\Sigma(1_{10})$	122.565	122.797	122.711
o	Σ	129.095	129.310	129.138
e	$\Sigma(1_{01})$	137.485	137.687	137.481
o	$\Sigma(1_{01})$	140.783	140.985	140.850
e	$\Sigma(1_{01})$	140.992	141.196	140.945
		$J = 1$		
o	$\Pi(1_{01})$	83.224	83.434	83.248
e	$\Pi(1_{01})$	83.454	83.664	83.478
o	$\Sigma(1_{01})$	95.309	95.518	95.300
e	$\Sigma(1_{01})$	98.834	99.047	99.020
o	$\Pi(1_{01})$	100.004	100.210	100.004
e	$\Pi(1_{01})$	100.899	101.110	101.063
o	$\Sigma(1_{01})$	115.389	115.602	115.047
e	$\Sigma(1_{10})$	123.879	124.111	124.025
e	$\Pi(1_{10})$	126.158	126.383	126.229
o	$\Pi(1_{10})$	126.261	126.486	126.324
e	$\Sigma(1_{11})$	130.346	130.561	130.414
e	$\Pi(1_{01})$	134.439	134.804	134.542
o	$\Pi(1_{01})$	134.596	135.147	134.634
o	$\Sigma(1_{01})$	138.501	138.702	138.505
e	$\Pi(1_{01})$	138.912	139.111	138.919
o	$\Pi(1_{01})$	139.077	139.276	139.074
e	Σ		141.847	141.698
o	$\Sigma(1_{01})$	142.015	142.218	141.972
		$J = 2$		
e	$\Pi(1_{01})$	85.596	85.806	85.619
o	$\Pi(1_{01})$	86.257	86.467	86.282
e	$\Sigma(1_{01})$	98.511	98.721	98.619
o	$\Sigma(1_{01})$	100.781	100.990	100.953
e	$\Pi(1_{01})$	102.588	102.794	102.588
o	$\Pi(1_{01})$	104.190	104.402	104.359
e	$\Delta(1_{01})$	110.678	110.890	110.727
o	$\Delta(1_{01})$	110.712	110.924	110.727
e	$\Sigma(1_{01})$	117.757	117.971	117.432
o	$\Sigma(1_{10})$	126.476	126.707	126.613
e	$\Delta(1_{10})$	126.858	127.081	126.878
o	$\Delta(1_{10})$	126.881	127.105	126.916
o	$\Pi(1_{10})$	129.049	129.273	129.109
e	$\Pi(1_{10})$	129.300	129.523	129.359
o	$\Sigma(1_{11})$	132.833	133.048	132.880
e	$\Pi(1_{01})$	135.858	136.066	135.897
o	$\Pi(1_{01})$	136.705	136.913	136.750
o	$\Pi(1_{01})$	139.904	140.104	139.936
e	$\Pi(1_{01})$	140.305	140.505	140.324
e	$\Sigma(1_{01})$	140.333	140.534	140.324
o	$\Delta(1_{01})$	142.044	142.242	142.061
e	$\Delta(1_{01})$	142.079	142.277	142.090

was made such as in our calculations, the character *ortho* or *para* of the rovibrational states could be determined from the expectation value of the grid population of the θ DOF. In other words the average value $\langle j \rangle$ of the rovibrational state where j is the angular momentum quantum number of the H$_2$ fragment. As it is well known for H$_2$, *para* and *ortho* states have respectively an even and odd j progression and therefore the value of $\langle j \rangle$ provides the necessary information to differentiate the states. Alternatively, using the Extended Legendre DVR filtered with *even* or *odd* functions could also allow one to differentiate pH$_2$ from oH$_2$ states. Third, the j of the dominant $j_{k_a k_c}$ use in the assignment can be determined from the expectation value of the grid population of the β DOF. Finally, as an alternative to all the previous methods, one could use projection methods like the one described by Wang and Carrington[23] to assign the states.

4. Conclusion

We report calculations of rovibrational energies on the H$_2$O-H$_2$ system in the rigid rotor approximation, obtained with the MCTDH algorithm on the Valiron PES[25]. Our results are found to be in very close agreement with the values previously reported. The calculations performed here with the MCTDH program are relatively fast, computationally cheaper and relatively easier to implement than

standard calculations and therefore appear as a bright prospect for the investigation of similar or other even more complex systems. Additionally, the extension to full dimensionality (9D) calculations on this system can be easily implemented and performed at a lower cost than other traditional methods, even though it may become more difficult to implement the symmetry in higher dimensionality. This work opens the path to a systematic study of various similar systems[50] and is an important step towards our study of H_2O+H_2 collisions which will be presented in a future paper.

Acknowledgment

References

[1] R. Bukowski, K. Szalewicz, G. C. Groenenboom, A. Van der Avoird, Predictions of the properties of water from first principles, Science 315 (5816) (2007) 1249–1252.

[2] X. Huang, B. J. Braams, J. M. Bowman, R. E. Kelly, J. Tennyson, G. C. Groenenboom, A. van der Avoird, New ab initio potential energy surface and the vibration-rotation-tunneling levels of $(H_2O)_2$ and $(D_2O)_2$, J. Chem. Phys. 128 (3) (2008) 034312.

[3] A. Shank, Y. Wang, A. Kaledin, B. J. Braams, J. M. Bowman, Accurate ab initio and hybrid potential energy surfaces, intramolecular vibrational energies, and classical ir spectrum of the water dimer, J. Chem. Phys. 130 (14) (2009) 144314.

[4] Y. Wang, X. Huang, B. C. Shepler, B. J. Braams, J. M. Bowman, Flexible, ab initio potential, and dipole moment surfaces for water. I. Tests and applications for clusters up to the 22-mer, J. Chem. Phys. 134 (9) (2011) 094509.

[5] G. R. Medders, A. W. Gtz, M. A. Morales, P. Bajaj, F. Paesani, On the representation of many-body interactions in water, J. Chem. Phys. 143 (2015) 104102.

[6] G. A. Cisneros, K. T. Wikfeldt, L. Ojame, J. Lu, Y. Xu, H. Torabifard, A. P. Bartk, G. Csányi, V. Molinero, F. Paesani, Modeling Molecular Interactions in Water: From Pairwise to Many-Body Potential Energy Functions, Chem. Rev. 116 (2016) 7501–7528.

[7] F. Paesani, Getting the right answers for the right reasons: toward redictive molecular simulations of water with many-body potentials, Acc. Chem. Res. 49 (2016) 1844–1851.

[8] G. R. Medders, F. Paesani, Infrared and Raman Spectroscopy of Liquid Water through "First-Principles" Many-Body Molecular Dynamics, J. Chem. Theory Comput. 11 (2015) 1145.

[9] G. R. Medders, F. Paesani, Many-body convergence of the electrostatic properties of water, J. Chem. Theory Comput. 9 (2013) 4844.

[10] X.-G. Wang and T. Carrington Jr., Using monomer vibrational wavefunctions to compute numerically exact (12D) rovibrational levels of water dimer, J. Chem. Phys. 148 (2018) 074108.

[11] V. Babin, C. Leforestier, F. Paesani, Development of a first principles water potenital with flexible monomers: Dimer potential energy surface, J. Chem. Theory Comput. 9 (2013) 5395.

[12] T. R. Philips, S. Maluendes, S. Green, Collision dynamics for an asymmetric top rotor and a linear rotor: Coupled channel formalism and application to $H_2O–H_2$, J. Chem. Phys. 102 (1995) 6024.

[13] M. L. Dubernet, A. Grosjean, Collisional excitation rates of H_2O with H_2. I. Pure rotational excitation rates with para-H_2 at very low temperature, Astron. & Astrophys. 390 (2002) 793–800.

[14] A. Faure, N. Crimier, C. Ceccarelli, P. Valiron, L. Wiesenfeld, M. L. Dubernet, Quasi-classical rate coefficient calculations for the rotational (de)excitation of H_2O by H_2, Astron. & Astrophys. 472 (2007) 1029–1035.

[15] M. L. Dubernet, F. Daniel, A. Grosjean, C. Y. Lin, Rotational excitation of ortho-H_2O by para-H_2 (j_2=0, 2, 4, 6, 8) at high temperature, Astron. & Astrophys. 497 (2009) 911–925.

[16] Y. Scribano, A. Faure, L. Wiesenfeld, Communication: Rotational excitation of interstellar heavy water by hydrogen molecules, J. Chem. Phys. 133 (2010) 231105.

[17] Y. Scribano, A. Faure, D. Lauvergnat, Rotational excitation of H_2O by para-H_2 from an adiabatically reduced dimensional potential, J. Chem. Phys. 136 (2012) 094109.

[18] W. L. Mao, C. A. Koh, E. D. Sloan, Clathrate hydrates under pressure, Phys. Today 60 (2007) 42.

[19] F. Schüth, Hydrogen and hydrates, Nature 434 (2005) 712.

[20] Z. Homayoon, R. Conte, C. Qu, J. M. Bowman, Full-dimensional, high-level ab initio potential energy surfaces for $H_2(H_2O)$ and $H_2(H_2O)_2$ with application to hydrogen clathrate hydrates, J. Chem. Phys. 143 (8) (2015) 084302.

[21] M. Xu, Y. Elmatad, F. Sebastianelli, J. W. Moskowitz, Z. Bačić, Hydrogen molecule in the small dodecahedral cage of a clathrate hydrate: Quantum five-dimensional calculations of the coupled translation-rotation eigenstates, J. Phys. Chem. B 110 (2006) 24806.

[22] A. Powers, Y. Scribano, D. Lauvergnat, E. Mebe, D. Benoit, Z. Bačić, The effect of the condensed-phase environment on the vibrational frequency shift of a hydrogen molecule inside clathrate hydrates, J. Chem. Phys. 148 (2018) 14430.

[23] X.-G. Wang and T. Carrington Jr., Theoretical study of the rovibrational spectrum of H_2O-H_2, J. Chem. Phys. 134 (4) (2011) 044313.

[24] A. van der Avoird, D. Nesbitt, Rovibrational states of the H_2O-H_2 complex: An ab initio calculation, J. Chem. Phys. 134 (4) (2011) 044314.

[25] P. Valiron, M. Wernli, A. Faure, L. Wiesenfeld, C. Rist, S. Kedžuch, J. Noga, R12-calibrated $H_2O–H_2$ interaction: Full dimensional and vibrationally averaged potential energy surfaces, J. Chem. Phys. 129 (13) (2008) 134306.

[26] S. Ndengué, R. Dawes, F. Gatti, H. D. Meyer, Atom-Triatom Rigid Rotor Inelastic Scattering with the MultiConfiguration Time Dependent Hartree approach, Chem. Phys. Lett. 668 (2017) 42.

[27] V. Buch, Treatment of rigid bodies by diffusion Monte Carlo: Application to the para-$H_2 \cdots H_2O$ and ortho-$H_2 \cdots H_2O$ clusters, J. Chem. Phys. 97 (1) (1992) 726–729.

[28] D. M. Benoit, D. C. Clary, Quantum simulation of phenol-water clusters, J. Phys. Chem. A 104 (23) (2000) 5590–5599.

[29] A. Viel, M. V. Patel, P. Niyaz, B. K. Whaley, Importance sampling in rigid body diffusion monte carlo, Comp. Phys. Com. 145 (1) (2002) 24–47.

[30] R. E. Kelly, J. Tennyson, G. C. Groenenboom, A. van der Avoird, Water dimer vibration–rotation tunnelling levels from vibrationally averaged monomer wavefunctions, J. Quant. Spectro. Rad. Trans. 111 (9) (2010) 1262–1276.

[31] D. M. Benoit, Xdmc, Quantum Diffusion Monte Carlo code (1999).

[32] D. M. Benoit, D. C. Clary, Quaternion formulation of diffusion quantum monte carlo for the rotation of rigid molecules in clusters, J. Chem. Phys. 113 (13) (2000) 5193–5202.

[33] H. D. Meyer, F. Gatti, G. A. Worth (Eds.), Multidimensional Quantum Dynamics: MCTDH Theory and Applications, Wiley-VCH: Weinheim, 2009.

[34] M. H. Beck, A. Jäckle, G. A. Worth, H. D. Meyer, The multiconfiguration time-dependent Hartree (MCTDH) method: a highly efficient algorithm for propagating wavepackets, Phys. Rep. 324 (2000) 1–105.

[35] G. Brocks, A. V. D. Avoird, B. T. Sutcliffe, J. Tennyson, Quantum dynamics of non-rigid systems comprising two polyatomic fragments, Mol. Phys. 50 (1983) 1025.

[36] F. Gatti, C. Iung, Exact and constrained kinetic energy operators for polyatomic molecules: The polyspherical approach, Phys. Rep. 484 (1) (2009) 1–69.

[37] C. Leforestier, Grid method for the Wigner functions. Application to the van der Waals system Ar–H_2O, J. Chem. Phys. 101 (9) (1994) 7357–7363.

[38] A. Jäckle, H. D. Meyer, Product representation of potential energy surfaces, J. Chem. Phys. 104 (1996) 7974–7984.

[39] A. Jäckle, H. D. Meyer, Product representation of potential energy surfaces. II, J. Chem. Phys. 109 (1998) 3772–3779.

[40] G. Worth, M. Beck, A. Jäckle, H. D. Meyer, The MCTDH Package, Version 8.2, (2000), University of Heidelberg, Heidelberg, Germany. H.-D. Meyer, Version 8.3 (2002), Version 8.4 (2007), O. Vendrell and H.-D. Meyer, Version 8.5 (2011), See http://mctdh.uni-hd.de (2007).

[41] D. Peláez, H.-D. Meyer, The multigrid POTFIT (MGPF) method: Grid representations of potentials for quantum dynamics of large systems, J. Chem. Phys. 138 (1) (2013) 014108.

[42] F. Otto, Multi-layer Potfit: An accurate potential representation for efficient high-dimensional quantum dynamics, J. Chem. Phys. 140 (1) (2014) 014106.

[43] M. Schröder, H.-D. Meyer, Transforming high-dimensional potential energy surfaces into sum-of-products form using Monte Carlo methods, J. Chem. Phys. 147 (6) (2017) 064105.

[44] L. J. Doriol, F. Gatti, C. Iung, H.-D. Meyer, Computation of vibrational energy levels and eigenstates of fluoroform using the multiconfiguration time-dependent hartree method, J. Chem. Phys. 129 (22) (2008) 224109.

[45] H.-D. Meyer, F. Le Quéré, C. Léonard, F. Gatti, Calculation and selective population of vibrational levels with the Multiconfiguration Time-Dependent Hartree (MCTDH) algorithm, Chem. Phys. 329 (2006) 179–192.

[46] R. Kosloff, H. Tal-Ezer, A direct relaxation method for calculating eigenfunctions and eigenvalues of the Schrödinger equation on a grid, Chem. Phys. Lett. 127 (1986) 223–230.

[47] H. D. Meyer, G. A. Worth, Quantum molecular dynamics: propagating wavepackets and density operators using the multiconfiguration time-dependent Hartree method, Theor. Chem. Acc. 109 (2003) 251–267.

[48] S. Sukiasyan, H. D. Meyer, Reaction Cross Sections for the $H+D_2(\nu_0=1) \rightarrow HD+D$ and $D+H_2(\nu_0=1) \rightarrow DH+H$ Systems. A Multiconfiguration Time-Dependent Hartree (MCTDH) Wave Packet Propagation Study, J. Chem. Phys. 116 (2002) 10641–10647.

[49] S. A. Ndengue, R. Dawes, F. Gatti, H.-D. Meyer, Resonances of HCO Computed Using an Approach Based on the Multiconfiguration Time-Dependent Hartree Method, J. Phys. Chem. A 119 (2015) 12043.

[50] Y. Kalugina, A. Faure, A. van der Avoird, K. Walker, F. Lique, Interaction of H_2O with CO: potential energy surface, bound states and scattering calculations, Phys. Chem. Chem. Phys. 20 (8) (2018) 5469–5477.